

# Fabrication of silicon carbide composites with carbon nanofiber addition and their fracture toughness

Jumpei Kita · Hiroshi Suemasu · Ian J. Davies ·  
Seiichiro Koda · Kiyoshi Itatani

Received: 4 December 2009 / Accepted: 3 June 2010 / Published online: 17 June 2010  
© Springer Science+Business Media, LLC 2010

**Abstract** The authors have examined the fabrication conditions of SiC composites containing carbon nanofiber, i.e., vapor-grown carbon nanofiber (VGCF), to enhance the fracture toughness. Commercially available ultrafine SiC powder (specific surface area:  $47.5 \text{ m}^2 \text{ g}^{-1}$ ) was mixed with VGCF and sintering aid in the  $\text{Al}_4\text{C}_3\text{-B}_4\text{C}$  system. Approximately 1.5 g of the mixture was uniaxially pressed at 50 MPa to obtain a compact with a diameter of 20 mm and a thickness of approximately 1.5 mm. The resulting compact was hot-pressed at 1800 °C for 1 h in Ar atmosphere under a pressure of 62 MPa. The relative density of hot-pressed SiC composite decreased from 98.0 to 96.3%, whereas the fracture toughness was enhanced from 3.8 to 5.2 MPa  $\text{m}^{1/2}$ , as the amount of VGCF increased from 0 to 6 mass%. Furthermore, an acid treatment of VGCF was conducted to enhance its dispersibility within the SiC matrix, owing to the formation of  $\text{COO}^-$  groups on the VGCF surface. As a result of this treatment, the relative density and fracture toughness of hot-pressed SiC composite with 6 mass% acid-treated VGCF addition increased to 99.0% and 5.7 MPa  $\text{m}^{1/2}$ , respectively.

## Introduction

Silicon carbide (SiC) ceramics are being used for high-temperature materials, because they have several characteristic properties, such as high elastic modulus and hardness, excellent thermal and chemical stabilities, low thermal and electrical conductivities, and relatively low thermal expansion coefficients [1]. However, when compared to the case of silicon nitride ( $\text{Si}_3\text{N}_4$ ), the practical application of SiC ceramics has been limited due to their relatively low fracture toughness [1]. One method to overcome this problem has been the development of SiC-based composites containing continuous inorganic fiber; however, the progress in this area has been hampered due to their relatively high cost [2, 3]. An alternative avenue of research has been the utilization of composites containing short fibers, allowing for modest increases in fracture toughness [4, 5] combined with simple fabrication processing and comparatively low cost (at least when compared to continuous fiber SiC-based composites).

In addition to this, recent years have noted a growing interest in carbon nanofiber (CNF) due to its excellent chemical, physical, and mechanical properties [6]. Therefore, CNF has been used as composite reinforcement fiber within polymer and ceramic matrices to take advantage of these characteristics [7].

In this study, the authors have examined the fabrication conditions of SiC composites containing CNF, i.e., vapor-grown carbon nanofiber (VGCF), with the main aim being to enhance the fracture toughness. VGCF was chosen as the reinforcement due to its extremely strong nano-sized structure allowing the manufacture of composites with extremely high strength and low mass [8]. However, the utilization of VGCF has been hampered by one main issue, namely the problem of fiber aggregation due to strong van

---

J. Kita · S. Koda · K. Itatani (✉)  
Department of Materials and Life Sciences, Sophia University,  
7-1, Kioi-cho, Chiyoda-ku, Tokyo 102-8554, Japan  
e-mail: itatani@sophia.ac.jp

H. Suemasu  
Department of Engineering and Applied Sciences, Sophia  
University, 7-1, Kioi-cho, Chiyoda-ku, Tokyo 102-8554, Japan

I. J. Davies  
Department of Mechanical Engineering, Curtin University of  
Technology, GPO Box U1987, Perth, WA 6845, Australia

der Waals interactions [9], with this issue being anticipated to limit the relative density and mechanical strength of resulting SiC composite. Therefore, reductions in the tendency for fiber aggregation would appear to be essential for the achievement of high mechanical properties due to the improved dispersion of fibers within the SiC matrix.

One method utilized by the authors in the present work to enhance the dispersibility of VGCF within the SiC matrix was modification of the VGCF surface, i.e., formation of carboxyl groups on the fiber surface by acid treatment. It was expected that VGCF containing carboxyl groups may be easily dispersed in polar solvents such as acetone, due to the addition of such a hydrophilic group [10, 11].

### Experimental procedure

The acid treatment of VGCF (Showa Denko, Tokyo, Japan) was carried out to modify the fiber surface. The VGCF (0.5 g) was placed into a mixture of concentrated sulfuric and nitric acids (volume: 25 and 75 cm<sup>3</sup>, respectively) and ultrasonicated for 1 h. Following this, the mixture was refluxed for 24 h at 40–60 °C and finally washed with distilled water and filtered off.

Ultrafine  $\beta$ -SiC powder (specific surface area: 47.5 m<sup>2</sup> g<sup>-1</sup>) (Sumitomo Osaka Cement, Tokyo, Japan), Al<sub>4</sub>C<sub>3</sub> (specific surface area: 5.69 m<sup>2</sup> g<sup>-1</sup>) (Nilaco, Tokyo), and B<sub>4</sub>C (specific surface area: 6.70 m<sup>2</sup> g<sup>-1</sup>) (Denki Kagaku Kogyo, Tokyo) were used as starting powders in this study. Al<sub>4</sub>C<sub>3</sub> (8 mass%) and B<sub>4</sub>C (2 mass%) were added to the SiC powder as sintering aids and mixed in the presence of acetone using an alumina mortar and pestle. Following this, up to 8 mass% of VGCF was added to the mixture; approximately 1.5 g of the resulting powder was then uniaxially pressed at 50 MPa and isostatically pressed at 100 MPa to form a compact with a diameter of 20 mm and a thickness of approximately 1.5 mm. The compact was hot-pressed at 1800 °C for 1 h under a pressure of 62 MPa in an argon (Ar) atmosphere with the heating rate being 30 °C min<sup>-1</sup> to 1100 °C and then 10 °C min<sup>-1</sup> to 1800 °C with the compact being furnace-cooled.

Crystalline phases were identified using an X-ray diffractometer (XRD; Model RINT2000PC, Rigaku, Tokyo) with monochromatic CuK $\alpha$  radiation generated at 40 kV and 40 mA. The substitution groups on the VGCF surface were investigated using a Fourier transform infrared (FT-IR) spectra (FT-IR; IR Prestige-21, Shimadzu, Kyoto) by means of the KBr method. The dispersibility of VGCF in polar solution was evaluated using ultraviolet–visible (UV–vis) spectroscopy (V-550, JASCO, Tokyo). The phase changes during the heating of VGCF in air were examined

by differential thermal analysis and thermogravimetry (DTA-TG; Thermo Plus TG8120, Rigaku, Tokyo). The morphologies of acid-treated VGCF were observed using a transmission electron microscope (JEOL 2011; acceleration voltage, 200 kV).

The relative densities of the hot-pressed compacts were calculated by dividing the bulk density by true density. The bulk density was measured on the basis of mass and dimensions, whereas the true density was measured picnometrically at 25 °C, using hexane as a replacement liquid after the specimen had been pulverized with an alumina mortar and pestle.

Fracture toughness measurements were carried out on rectangular specimens of dimension 15 × 3 × 1.5 mm<sup>3</sup> cut from the hot-pressed compacts using a diamond saw and then polished to a 1  $\mu$ m surface finish. Each specimen was cut such that the load was applied parallel to the direction of hot pressing. The fracture toughness,  $K_{IC}$ , was determined using the single-edge notched beam (SENB) technique for specimens containing a notch (depth 1 mm and width 0.3 mm) introduced using a diamond saw. A span and cross-head speed of 10 mm and 0.5 mm min<sup>-1</sup>, respectively, were utilized with each  $K_{IC}$  value being calculated from the average of five specimens.

The fracture surfaces of specimens were investigated using a field-emission scanning electron microscope (FE-SEM; Model S-4500, Hitachi, Tokyo; acceleration voltage, 5 kV), after the specimen surface had been coated with Pt–Pd using an ion coater (Model E-1030, Hitachi, Tokyo) to avoid charging effects.

### Results and discussion

#### Properties of as-received and acid-treated VGCF

First, FE-SEM and TEM micrographs of the as-received VGCF are presented in Fig. 1. The mean diameter and length of the VGCF were determined to be 50 nm and 10  $\mu$ m, respectively. As anticipated, the VGCF was entangled so as to form agglomerates [12]. The electron diffraction pattern (Fig. 1b) showed the presence of bright distinct spots, indicating the VGCF to be crystalline in nature. In addition, the specific surface area of VGCF measured by the BET method was found to be 13.0 m<sup>2</sup> g<sup>-1</sup>.

As mentioned previously, the acid treatment of VGCF was conducted to modify the surface. XRD patterns following the acid treatment of VGCF in a mixed solution of H<sub>2</sub>SO<sub>4</sub> and HNO<sub>3</sub> at a temperature between 40 and 60 °C are shown in Fig. 2, together with FE-SEM micrographs. Whereas XRD patterns of the VGCF acid-treated at 40 and 50 °C indicated the presence of a sharp main diffraction

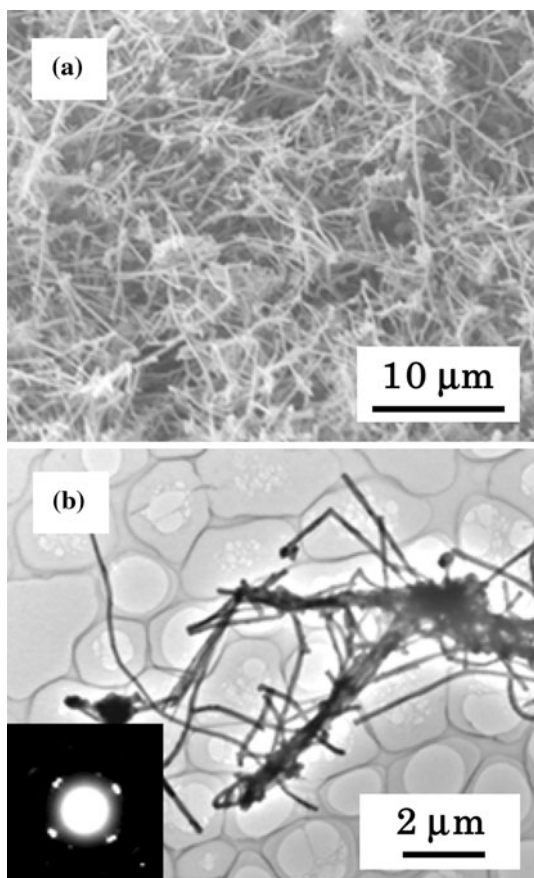


**Fig. 1** FE-SEM (a) and TEM micrographs and electron diffraction pattern (b) of as-received VGCF

reflection at  $26.6^\circ$ , the equivalent reflection of VGCF acid-treated at  $60^\circ\text{C}$  was broader. Such results may be explained by assuming that the acid treatment at  $60^\circ\text{C}$  for 24 h altered the crystalline structure of VGCF, due to the significant surface damage.

The VGCF acid-treated at 40 and  $50^\circ\text{C}$  kept their original shapes. However, in contrast to this, FE-SEM micrographs of the VGCF acid-treated at  $60^\circ\text{C}$  for 24 h indicated the presence of substantial damage to the fibers. It was found that the VGCF shape was changed with increasing refluxing temperature from 40 to  $60^\circ\text{C}$ . These results are consistent with that noted by previous research which stated that the severe acid treatment of VGCF leads to complete oxidation and consumption of defect-rich areas [13]. Other researchers have also reported that carbon nanotubes acid-treated under severe conditions tend to break up into fragments [14].

FT-IR spectra for each refluxing temperature, together with a typical TEM micrograph, are shown in Fig. 3. The FT-IR spectra contained absorption peaks at  $1550$  and  $1340\text{ cm}^{-1}$  with these peaks being assigned to  $\text{COO}^-$  asymmetric and symmetric stretching vibrations, respectively [15]. The TEM micrograph of the VGCF acid-treated

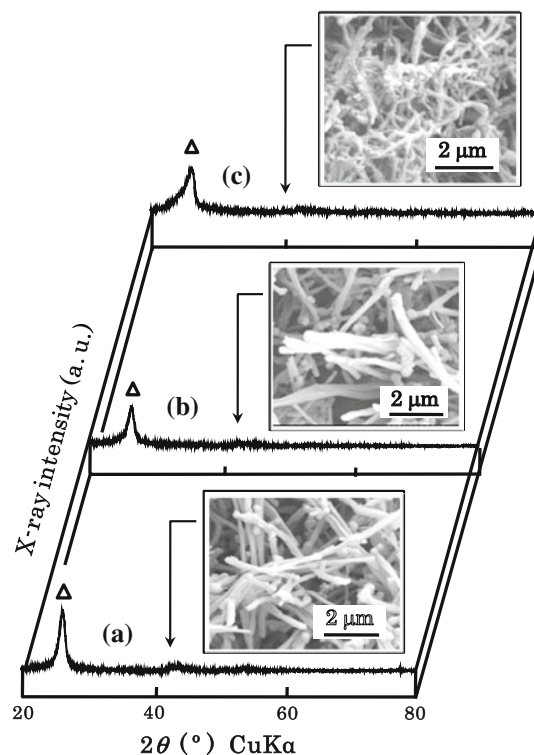


**Fig. 2** XRD patterns of VGCF acid-treated in the mixed solution of  $\text{H}_2\text{SO}_4$  and  $\text{HNO}_3$  at (a)  $40^\circ\text{C}$ , (b)  $50^\circ\text{C}$ , and (c)  $60^\circ\text{C}$  for 24 h, together with their FE-SEM micrographs. filled triangle C

at  $50^\circ\text{C}$  for 24 h indicated the presence of surface defects due to the acid treatment. In light of this, functional  $\text{COO}^-$  groups are believed to have been added to the VGCF surface, in addition to the formation of defects (see typical image regarding the bonding of  $\text{COO}^-$  groups to the VGCF).

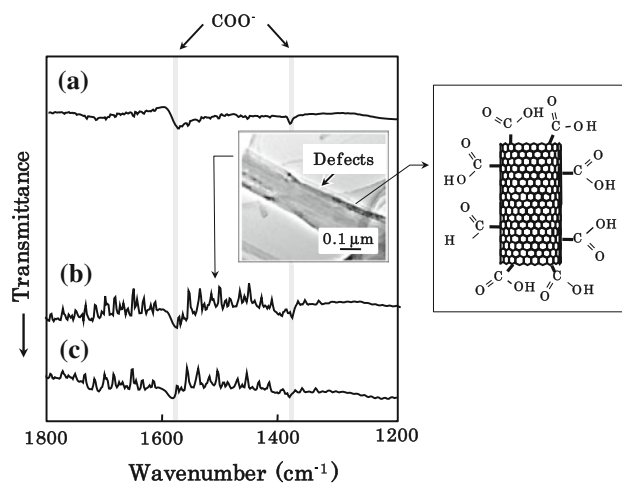


**Fig. 3** FT-IR spectra of VGCF acid-treated in a mixed solution of  $\text{H}_2\text{SO}_4$  and  $\text{HNO}_3$  at (a)  $40^\circ\text{C}$ , (b)  $50^\circ\text{C}$ , and (c)  $60^\circ\text{C}$  for 24 h, together with a typical TEM micrograph and image showing the chemical bonding of carboxyl groups to the VGCF surface

On the basis of the XRD and FT-IR results, we selected the optimum acid-treated temperature for the addition of carboxyl groups to be 50 °C. The specific surface area of VGCF acid-treated at 50 °C for 24 h was measured using the BET method and calculated to be  $34.9 \text{ m}^2 \text{ g}^{-1}$ . Compared to the case of as-received VGCF ( $13.0 \text{ m}^2 \text{ g}^{-1}$ ), the specific surface area of the acid-treated VGCF was therefore significantly enhanced. Toebes et al. [13] had previously attributed such an increase of specific surface area for VGCF to three effects, namely, surface roughness, fragmentation, and opening of the fiber inner tubes. In this study, since fragmentation and opening of the VGCF were not observed from FE-SEM and TEM micrographs, the increase in specific surface area is attributed to an increase in surface roughness.

The dispersibility of VGCF in the polar solvent was evaluated by means of UV–vis spectroscopy. Figure 4 illustrates the UV–vis spectra of the as-received and acid-treated VGCFs in acetone. Whereas the transmittance of the as-received VGCF was approximately 75%, the value was almost 0% in the case of acid-treated VGCF. In comparison to the as-received VGCF, therefore, the dispersibility of acid-treated VGCF may be significantly enhanced within polar solvents (e.g., acetone).

DTA–TG curves of as-received and acid-treated VGCFs are presented in Fig. 5. It was noted that the weight of as-received VGCF did not start to decrease until 600 °C and then continued decreasing upon further heating (Fig. 5a). The weight loss above 600 °C is attributed to the oxidation of the VGCF yielding carbon monoxide and dioxide. In contrast to this, the weight of the acid-treated

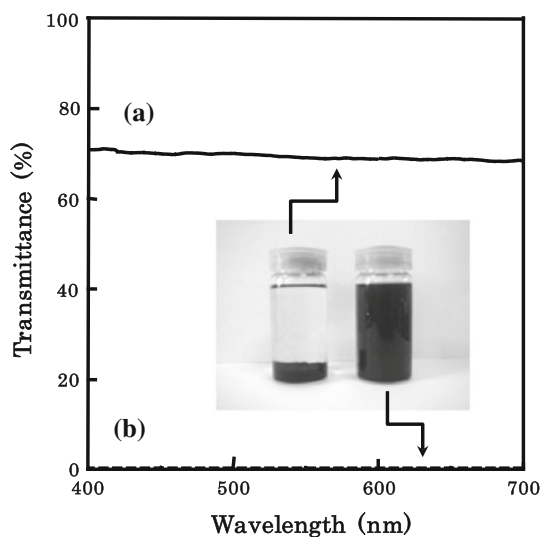


**Fig. 4** UV–vis spectra of (a) as-received VGCF and (b) VGCF acid-treated in a mixed solution of  $\text{H}_2\text{SO}_4$  and  $\text{HNO}_3$  at 50 °C for 24 h, together with a photograph illustrating the dispersion of VGCF in acetone

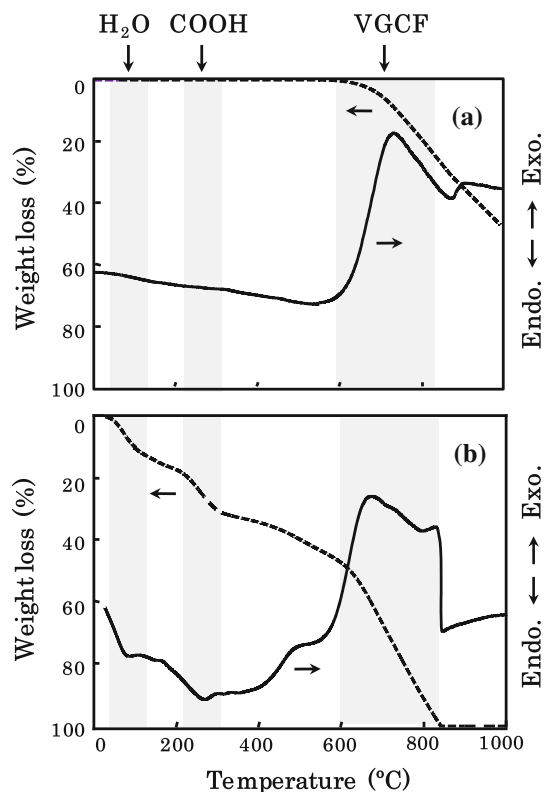


**Fig. 5** DTA–TG curves of (a) as-received VGCF and (b) VGCF acid-treated in a mixed solution of  $\text{H}_2\text{SO}_4$  and  $\text{HNO}_3$  at 50 °C for 24 h. Heating rate:  $10 \text{ }^\circ\text{C min}^{-1}$

VGCF decreased immediately upon heating (Fig. 5b). Such significant weight losses, especially below 300 °C, may be attributed to the elimination of physically adsorbed water (around 100 °C) together with the thermal decomposition of carboxyl groups above 200 °C.

#### Relative density and crystalline phases of SiC composite

The effect of VGCF addition on the relative density of SiC composite with VGCF addition (sintering aid: 8 mass%  $\text{Al}_4\text{C}_3$ , 2 mass%  $\text{B}_4\text{C}$ ) hot-pressed at 1800 °C for 1 h is shown in Fig. 6. The relative density gradually decreased from 98.0 to 93.5% as the amount of as-received VGCF addition increased from 0 to 8 mass% (Fig. 6a). The decrease in relative density of the SiC composite with increasing amount of VGCF was attributed to increasing amounts of residual porosity within the VGCF agglomerates in the SiC matrix.

In contrast to this, the relative density of SiC composite containing acid-treated VGCF gradually increased to reach a maximum of 99.0% at 4 mass% VGCF addition—further increases in VGCF content resulted in decreased relative density (Fig. 6b). A key result of this work was that, for any given amount of VGCF addition, the relative density of

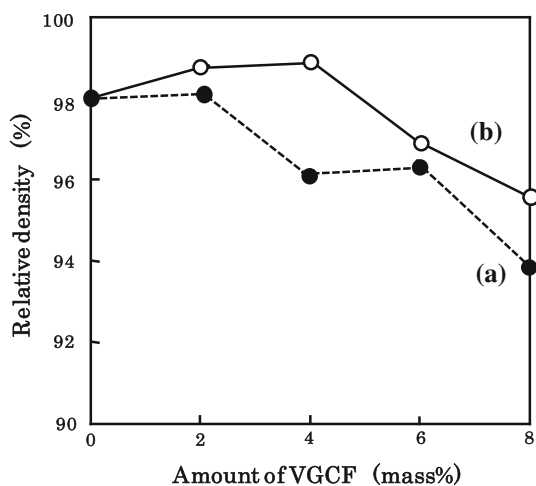


**Fig. 6** Effect of VGCF addition on the relative density of SiC composite hot-pressed at 1800 °C for 1 h under a pressure of 62 MPa in Ar atmosphere. (a) Addition of as-received VGCF, (b) addition of VGCF acid-treated in a mixed solution of H<sub>2</sub>SO<sub>4</sub> and HNO<sub>3</sub> at 50 °C for 24 h

SiC composite containing acid-treated VGCF was always higher when compared to that of the as-received VGCF case. This phenomenon is directly attributed to the increased dispersibility of VGCF within the SiC matrix due to the acid treatment, i.e., acid treatment of VGCF → enhanced dispersibility of VGCF in the polar solvent during composite manufacture → increased relative density of the SiC composite. Previous work by the authors [4] had indicated that higher relative density for discontinuous fiber-reinforced SiC composite had resulted in improved mechanical properties and, thus, it may be reasonable to expect a similar trend to exist in the present composites.

The effect of acid-treated VGCF addition on the crystalline phases present within hot-pressed SiC composite is shown in Fig. 7. Crystalline phases of  $\beta$ -SiC,  $\alpha$ -SiC, and C were detected in the SiC composites with 2–8 mass% VGCF addition. The  $\beta$ -SiC and C were attributed to the starting  $\beta$ -SiC and VGCF, respectively. With reference to the  $\alpha$ -SiC, Shinozaki and coworker [16, 17] have previously noted that crystalline SiC was transformed from  $\beta$  to  $\alpha$  above 1800 °C. Therefore, the presence of  $\alpha$ -SiC in the composites is attributed to the transformation of  $\beta$ -SiC during hot pressing. The lack of any minor phases attributed to the reaction between the sintering aids and/or SiC and VGCF was explained in terms of the sintering aids forming amorphous phases as is often the case in SiC ceramics.

#### Mechanical properties and microstructure of SiC composite

The effect of VGCF addition on the fracture toughness of hot-pressed SiC composite, together with typical FE-SEM micrographs showing the fracture surfaces, is shown in Fig. 8. In the case of the

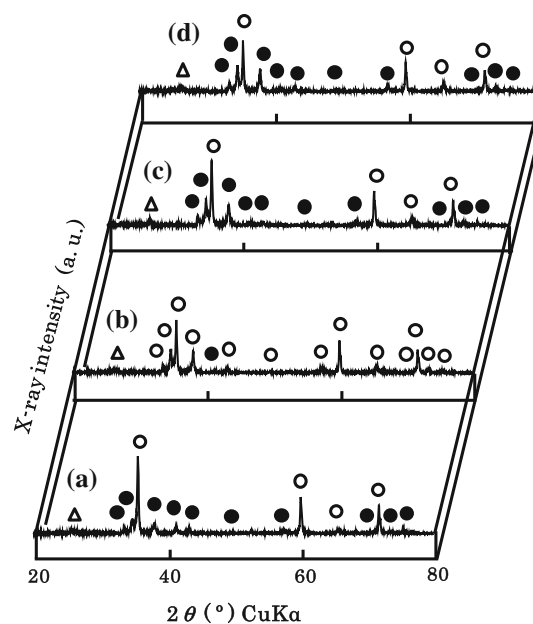


**Fig. 7** Effect of acid-treated VGCF addition on the crystalline phases of SiC composite hot-pressed at 1800 °C for 1 h under a pressure of 62 MPa in Ar atmosphere: (a) 2 mass%, (b) 4 mass%, (c) 6 mass%, (d) 8 mass%. Filled circle  $\alpha$ -SiC, open circle  $\beta$ -SiC, filled triangle C. Note that the VGCF was acid-treated in a mixed solution of H<sub>2</sub>SO<sub>4</sub> and HNO<sub>3</sub> at 50 °C for 24 h

as-received VGCF addition, the fracture toughness was 3.8 MPa m<sup>1/2</sup> for the SiC composite with no VGCF addition and gradually increased with increasing VGCF addition to reach 5.2 MPa m<sup>1/2</sup> for the case of 6 mass% VGCF addition. However, a further increase in the amount of VGCF addition to 8 mass% decreased the fracture toughness to 4.6 MPa m<sup>1/2</sup>. In the case of acid-treated VGCF addition, the fracture toughness gradually increased with

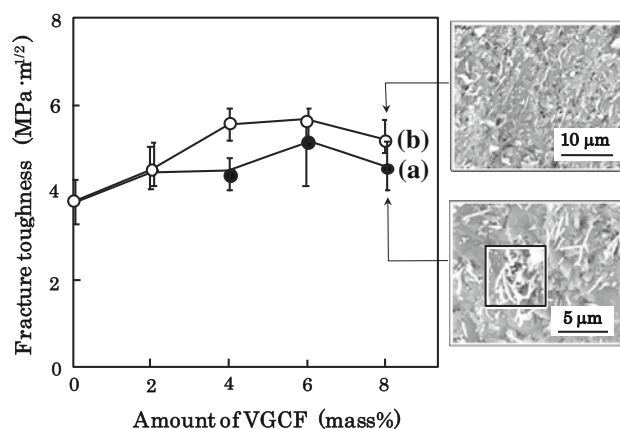


**Fig. 8** Effect of VGCF addition on the fracture toughness of SiC composite hot-pressed at 1800 °C for 1 h under a pressure of 62 MPa in Ar atmosphere, together with typical FE-SEM micrographs showing the fracture surfaces. (a) Addition of as-received VGCF, (b) addition of VGCF acid-treated in a mixed solution of H<sub>2</sub>SO<sub>4</sub> and HNO<sub>3</sub> at 50 °C for 24 h

increasing amount of VGCF addition and reach a maximum of  $5.7 \text{ MPa m}^{1/2}$  for the case of 4 mass% VGCF addition. Similar to the trend noted for relative densities, the fracture toughness values of SiC composites with acid-treated VGCF addition are consistently higher than those for as-received VGCF addition at any given amount of VGCF addition.

In order to better understand why the fracture toughness increased with increasing amounts of VGCF addition, the fracture surfaces of SiC composites were observed using FE-SEM. In contrast to the SiC composites containing as-received VGCF, FE-SEM micrographs for the SiC specimens with acid-treated VGCF addition indicated the absence of both agglomerated VGCF and significant porosity at the interface between matrix and VGCF. These morphological improvements, due to the enhanced dispersibility of VGCF in the SiC matrix, are believed to have improved the fracture toughness, similar to the trend noted for previously examined SiC-based composites [17].

The distribution of pull-out lengths at the fracture surface of SiC composites was measured to investigate the interaction of pull-out length and fracture toughness. The effect of acid treatment on the pull-out length distribution of VGCF in hot-pressed SiC composite, together with typical FE-SEM micrographs of the fracture surfaces, is shown in Fig. 9. The frequency of pull-out lengths for as-received VGCF (Fig. 9a) gradually decreased with increasing pull-out length up to approximately  $6 \mu\text{m}$  (mean length:  $3.25 \mu\text{m}$ ). In contrast to this, approximately 80% of the pulled-out fibers in the composite containing acid-treated VGCF possessed pull-out lengths of  $<3 \mu\text{m}$  (mean pull-out length:  $2.68 \mu\text{m}$ ). In many continuous fiber ceramic matrix composites, the existence of larger pull-out lengths is often associated with improved mechanical properties [18], whereas factors such as aspect ratio and volume fraction of the reinforcing phase are known to enhance the fracture toughness in discontinuous ceramic matrix composites [19–22]. Thus, in this study, the trend with regards to mean pull-out length (Fig. 9) and fracture toughness (Fig. 8) is opposite to that expected. However, a tentative explanation for this phenomenon may be attributed to the surface roughness of the VGCF, as previously mentioned, being increased following acid treatment. It would be reasonable to assume that the increased surface roughness may also lead to a higher surface friction (i.e., fiber/matrix interface shear strength,  $\tau$ ). For such a situation, it is therefore proposed that smaller pull-out lengths of acid-treated VGCF with higher  $\tau$  may have resulted in a larger overall frictional traction during crack propagation (and hence absorb greater frictional energy) when compared to the case of larger pull-out lengths of as-received VGCF with lower  $\tau$ . This effect would also be aided by the improved densification of the SiC composite containing

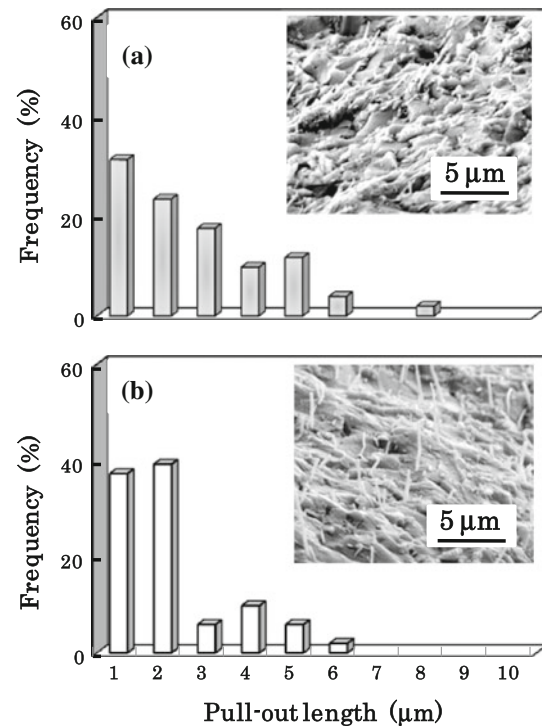


**Fig. 9** Effect of VGCF addition on the pull-out length at the fracture surface of SiC composite hot-pressed at  $1800 \text{ }^\circ\text{C}$  for 1 h under a pressure of 62 MPa in Ar atmosphere, together with typical FE-SEM micrographs showing the fracture surfaces. (a) Addition of as-received VGCF, (b) addition of VGCF acid-treated in a mixed solution of  $\text{H}_2\text{SO}_4$  and  $\text{HNO}_3$  at  $50 \text{ }^\circ\text{C}$  for 24 h

acid-treated VGCF. Consequently, the improvement of fracture toughness for SiC composite containing acid-treated VGCF could tentatively be explained in terms of the increased surface roughness of VGCF due to the acid treatment.

## Conclusions

Silicon carbide (SiC) composites with 0–8 mass% of acid-treated vapor-grown carbon nanofiber (VGCF) addition and 8 mass%  $\text{Al}_4\text{C}_3$  and 2 mass%  $\text{B}_4\text{C}$  sintering aid were fabricated using hot pressing at  $1800 \text{ }^\circ\text{C}$  for 1 h under a uniaxial pressure of 62 MPa. Results obtained from the densification behaviour, microstructure, and mechanical behaviour of the resulting SiC composites may be summarized as follows:

1. Whereas the relative density of SiC composite gradually decreased with increasing amount of as-received VGCF addition, the fracture toughness of SiC composite gradually increased with increasing amount of as-received VGCF addition. A maximum fracture toughness of  $5.2 \text{ MPa m}^{1/2}$  was achieved for the case of 6 mass% VGCF addition.

2. The acid treatment of VGCF was conducted to modify the VGCF surface. The VGCF acid-treated at 50 °C for 24 h was found to have essentially kept its original form with the addition of surface carboxyl groups and increased surface roughness. The acid-treated VGCF was found to be highly dispersed in the polar solvent (acetone).
3. The relative density and fracture toughness of the SiC composite with 4 mass% acid-treated VGCF addition attained 99.0% and 5.7 MPa m<sup>1/2</sup>, respectively, and this was directly attributed to enhanced dispersibility of the VGCF within the SiC matrix.
4. The distribution of pull-out length of VGCF at the fracture surface of the composite was measured to investigate the interaction of pull-out length and fracture toughness. The mean pull-out length for the as-received and acid-treated VGCF was 3.25 and 2.68 μm, respectively. The situation of smaller pull-out lengths producing large fracture toughness for the acid-treated VGCF composite was explained in terms of the increased roughness of the VGCF surface following acid treatment.

**Acknowledgement** The authors wish to thank Denki Kagaku Kogyo Co., Ltd. (Tokyo, Japan) for providing the B<sub>4</sub>C powder.

## References

1. Somiya S, Inomata Y (eds) (1991) Silicon carbide ceramics. Elsevier Science Publishing, New York
2. Zhu S, Mizuno M, Kagawa Y, Cao J, Nagano Y, Kaya H (1999) *J Am Ceram Soc* 82:117
3. Kameda T, Suyama S, Itou Y, Nishida K (1999) *J Ceram Soc Jpn* 107:622
4. Sato M, Itatani K, Tanaka T, Davies IJ, Koda S (2006) *J Mater Sci* 41:7466. doi:10.1007/s10853-006-0791-3
5. Hirota K, Hara H, Kato M (2007) *Mater Sci Eng* 485:216
6. Jacobsen RL, Tritt TM, Guth JR, Ehrlich AC, Gillespie DJ (1995) *Carbon* 33:1217
7. Maensiri S, Laokul P, Kinkawarnong J, Amornkitbamrung V (2007) *Mater Sci Eng* 447:44
8. Uchida T, Anderson DP, Minus ML, Kumar S (2006) *J Mater Sci* 41:5851. doi:10.1007/s10853-006-0324-0
9. Sun J, Gao L (2003) *Carbon* 41:1063
10. Tomonari Y, Murakami H, Nakashima N (2006) *Chem Eur J* 12:4027
11. Ros TG, van Dillen J A, Geus JW, Koningsberger DC (2002) *Chem Eur J* 5:2868
12. Itou Y, Kameda T, Nishida K, Umezawa M, Imai K, Ichikawa H (1998) *J Ceram Soc Jpn* 106:830
13. Toebes ML, van Heeswijk JMP, Bitter JH, van Dillen AJ, de Jong KP (2004) *Carbon* 42:307
14. Li YH, Wang S, Luan Z, Ding J, Xu C, Wu D (2003) *Carbon* 41:1057
15. Kubota S, Nishikiori H, Tanaka N, Endo M, Fujii T (2005) *J Phys Chem B* 109:23170
16. Shinozaki S, Williams RM, Juterbock BN, Donlon WT, Hangas J, Peters CR (1985) *Am Ceram Soc* 64:1389
17. Williams RM, Juterbock BN, Shinozaki S, Peters CR, Whalen TJ (1985) *J Am Ceram Soc* 64:1385
18. Davies IJ, Ishikawa T, Shibuya M, Hirokawa T (1999) *Comp Sci Technol* 59:801
19. Akatsu T, Tanabe Y, Yasuda E (1999) *J Mater Res* 14:1316
20. Suemasu H, Kondo A, Itatani K, Nozue A (2001) *Comp Sci Technol* 61:281
21. Zhou CR, Yu ZB, Krstic VD (2007) *J Eur Ceram Soc* 27:437
22. Krstic Z, Yu Z, Krstic VD (2007) *J Mater Sci* 42:5431. doi:10.1007/s10853-006-0826-9